Electronic Supplementary Information

Soft Gold Nanowire Sponge Antenna for Battery-Free Wireless Pressure Sensor

Kaixuan Wang,[a] Fenge Lin,[a] Daniel T. H. Lai,[b] Shu Gong,[a] Behailu Kibret,[c] Muhammad Ali,[c] Mehmet Rasit Yuce,[c] Wenlong Cheng*[a]

[a] Department of Chemical Engineering, Monash University, Clayton, Victoria 3800, Australia. E-mail: wenlong.cheng@monash.edu

[b] College of Engineering and Science, Victoria University, Victoria 8001, Australia

[c] Department of Electrical and Computer Systems Engineering, Monash University, Clayton, Victoria 3800, Australia

*Correspondence author. Email: W. L. Cheng (wenlong.cheng@monash.edu)

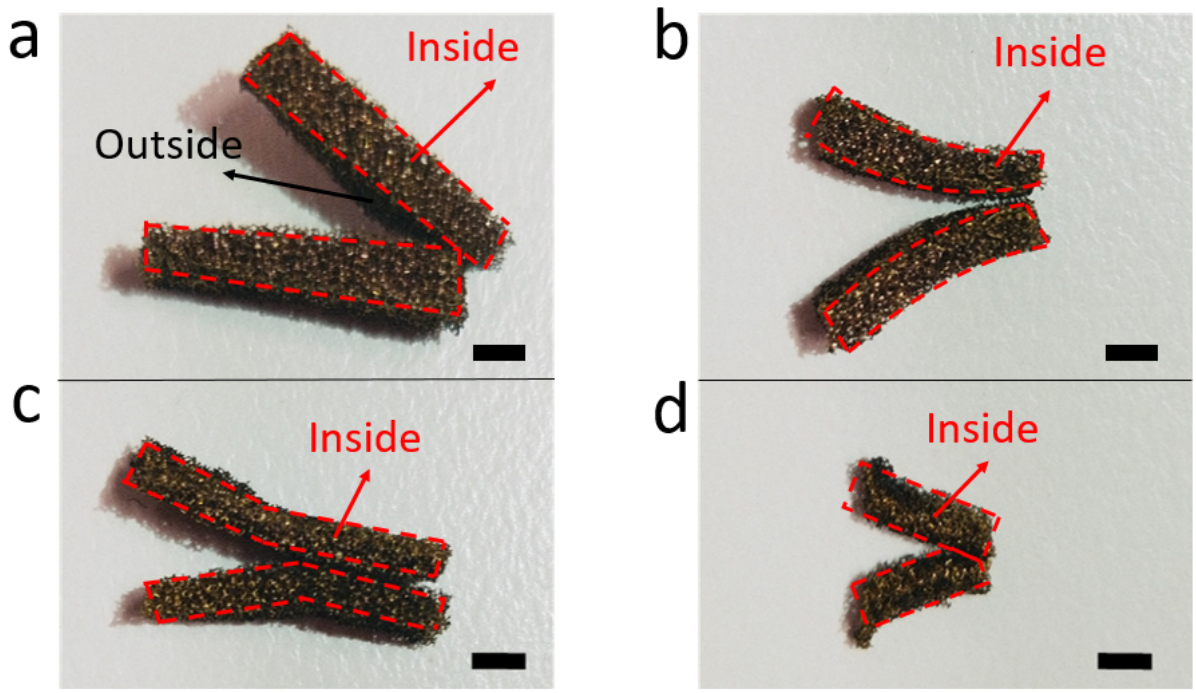

Figure S1 Four gold sponge samples were selected from four different batches. Each sample were cut into two pieces to display the growth of v-AuNWs inside the sponge (as shown in red dash frames). Both inside and outside of the sponge pieces are golden, which demonstrates the conformal coating of v-AuNWs on sponge skeleton. Scale bar: 2mm.

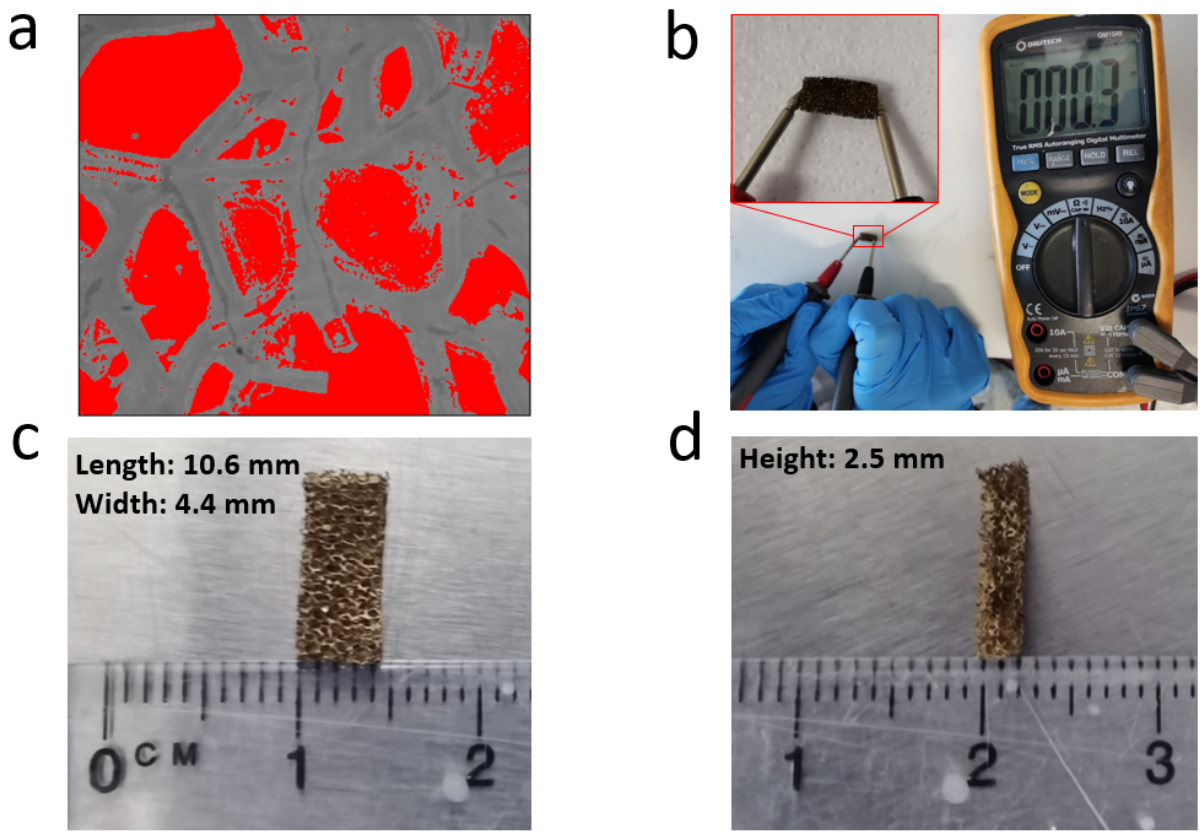

Figure S2 (a) Particles analysis image of Figure 1b. The pores are painted with red color by Image J. (b) Resistance test of a small piece sponge ribbon. (c-d) Top view and side view of the sponge ribbon shown in (b).

We did particles analysis of the sponge ribbon with the software (Image J). The parts in grey are the sponge skeletons; the parts in red are the pores inside the sponge. The sponge porosity of 42.42% was automatically calculated by Image J, which is the ratio between pores' area and the sum of sponge skeleton's area and pores' area.

For calculating the conductivity of gold sponge ribbon, we measured the resistance and dimension of a small piece ribbon (Figure S2b-d). The equations for calculating conductivity is

$$R = \rho \frac{L}{A}, \sigma = \frac{1}{\rho}$$

where R is the conductor resistance, L and A are the length and cross-section area of the conductor, ρ and σ are resistivity and conductivity of the conductor.

Because sponge has a 3D porous structure, the effective A should be width * height * (1 - porosity), namely 6.33 mm^2. Accordingly, the conductivity is ~ 5582 S/m.

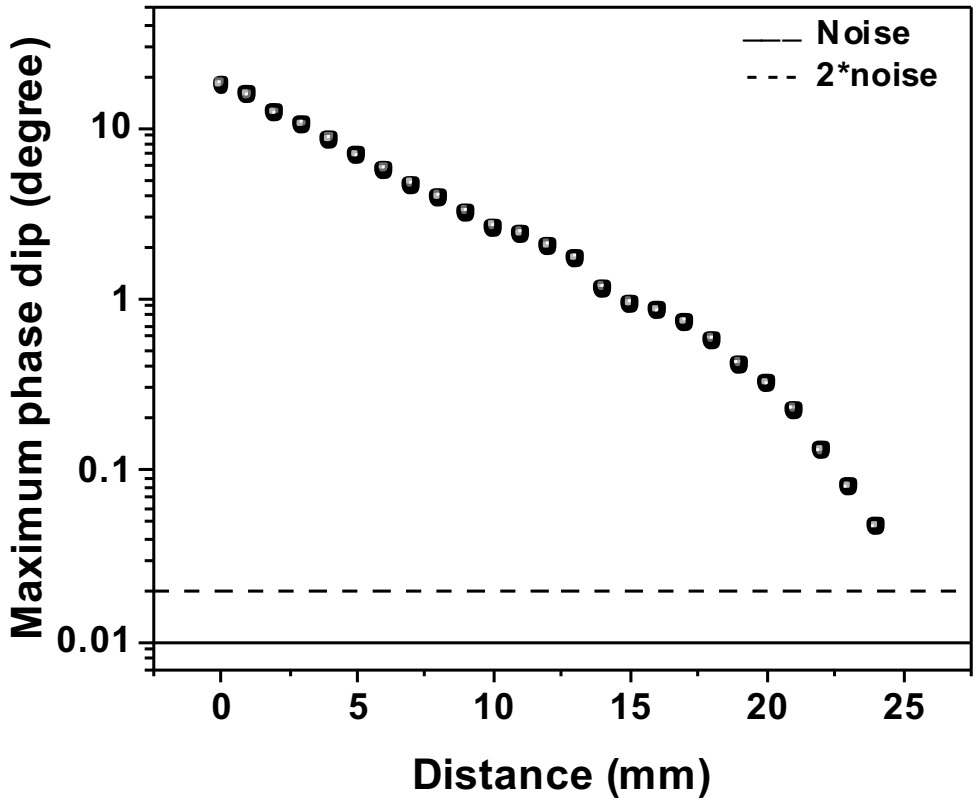

Figure S3 Measured maximum phase dip of reader coil versus the detection distance between the coil and sponge antenna. 0.01° is background noise level. The tested sponge antenna was encapsulated with Ecoflex and the sponge ribbon thickness is 8.5 mm.

For antenna performance characterization, 0.01° could be regarded as background noise level of phase dip signal.[1] The signal amplitude that is higher than this can be regarded as effective signal. It is noted that all the obtained signals' amplitude are higher than 2 times of noise signal level (detection distance from 0 to 24 mm), indicating that the data is reliable before the detection distance exceeding 24 mm. In addition, the detection distance in following tests are all 2 mm to ensure the good and consistent signal quality.

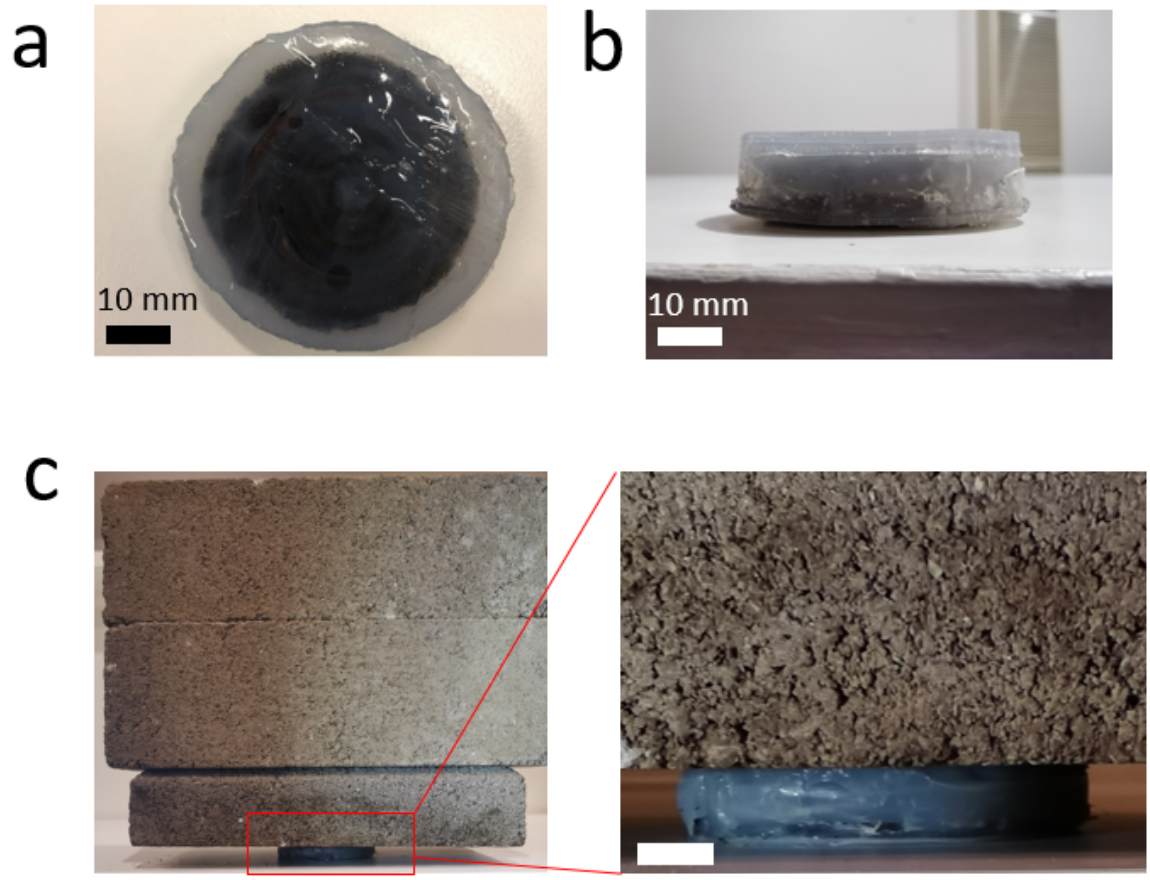

Figure S4 (a-b) Top view and side view of sponge antenna embedded in Ecoflex. (c) Shape deformation of the antenna under bricks with total weight of 8.2 kg. Scale bar: 10 mm.

In initial state, the diameter for this sponge antenna is 52 mm. The thickness of the antenna and inside sponge ribbon are 12 mm and 8.5 mm. Figure S4c is an optical image of the antenna under three bricks with a total weight of 8.2 kg. In this state, the thickness of the antenna is 11.1 mm, the diameter of the antenna is around 53.9 mm.

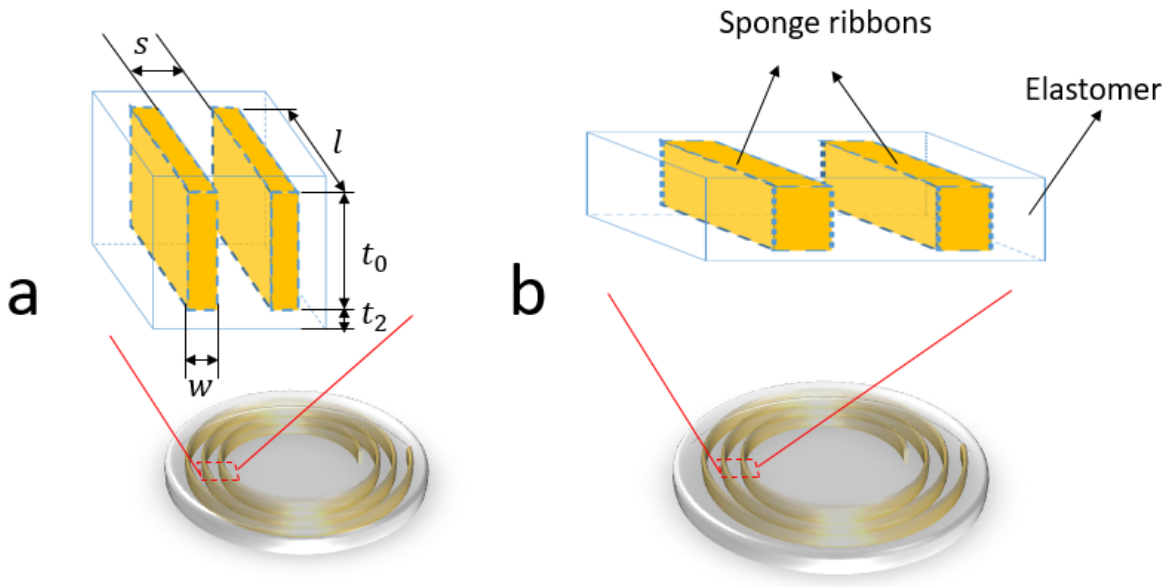

Figure S5 Sponge antenna under (a) Initial state and (b) Compression state.

Poisson effect, the phenomenon in which a material tends to expand in directions perpendicular to the direction of compression.

Poisson's ratio is a measure of the Poisson effect, which describes the expansion or contraction of a material in directions perpendicular to the direction of loading. The value of Poisson's ratio (v) is the negative of the ratio of transverse strain to axial strain.

Assuming that the material is stretched or compressed along the axial direction, then

$$v = -\frac{d\varepsilon_{trans}}{d\varepsilon_{axial}} = -\frac{d\varepsilon_y}{d\varepsilon_x} = -\frac{d\varepsilon_z}{d\varepsilon_x}$$

$$d\varepsilon_x = \frac{dx}{x},\ d\varepsilon_y = \frac{dy}{y}, d\varepsilon_z = \frac{dz}{z}$$

where ε_{trans} is transverse strain (negative for axial tension (stretching), positive for axial compression), ε_{axial} is axial strain (positive for axial tension, negative for axial compression).

$d\varepsilon_{x/y/z}$ is the length increase/decrease ratio of the material in x/y/z direction.

Applying this rule to sponge antenna, we can get

$$v = -\frac{d\varepsilon_s}{d\varepsilon_t} = -\frac{d\varepsilon_l}{d\varepsilon_t} = -\frac{d\varepsilon_w}{d\varepsilon_t}$$

Furthermore, since we have assumed that the Poisson's ratio of sponge antenna equals to that of Ecoflex, 0.5. Then we can get

$$d\varepsilon_s = d\varepsilon_l = d\varepsilon_w = -\frac{d\varepsilon_t}{2}$$

$$\frac{ds}{s} = \frac{dl}{l} = \frac{dw}{w} = -\frac{dt}{2t}$$

Therefore, after measuring the changes of thickness (dt), we can calculate the changes of

spacing (*ds*), length (*dl*) and width (*dw*) because we know the original value of thickness (*t*), spacing (*s*), length (*l*) and width (*w*). Then we can determine the ideal values of thickness (*t-dt*), spacing (*s+ds*), length (*l+dl*) and width (*w+dw*) under each applied pressure. These values are essential to simulation and theoretical analysis of the sponge antenna's capacitance, inductance and resonant frequency.

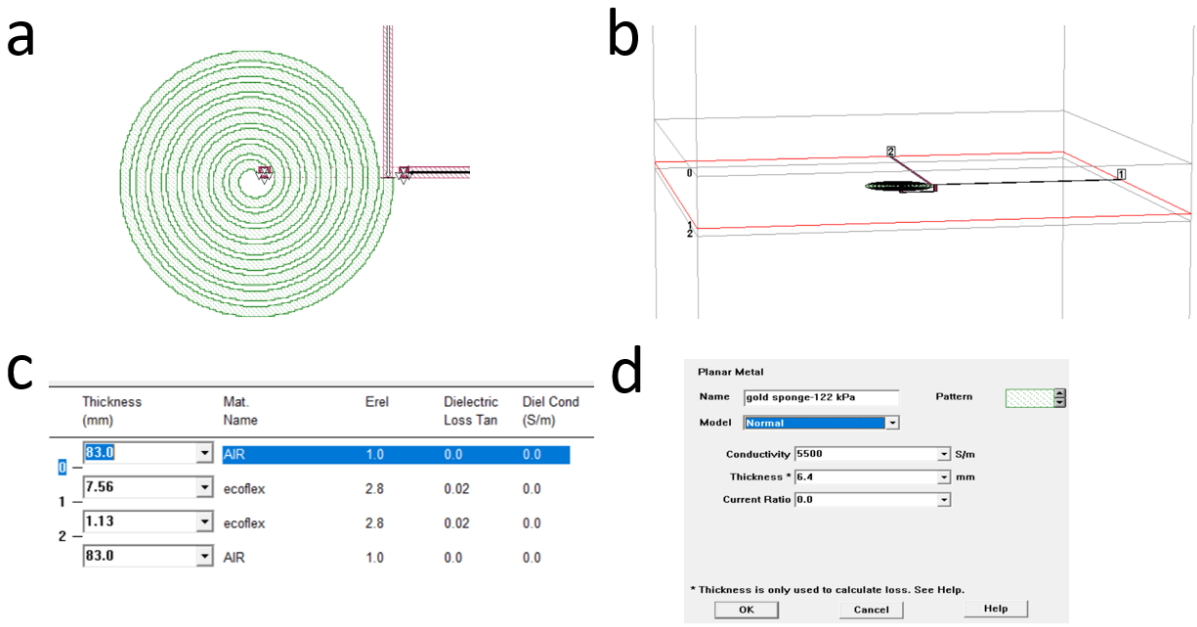

Figure S6 SONNET simulation. (a-b) 2D/3D view of antenna model for the gold sponge antenna embedded in Ecoflex (c-d) Dielectric layers and metal types setup for the sponge antenna under pressure of 122 kPa.

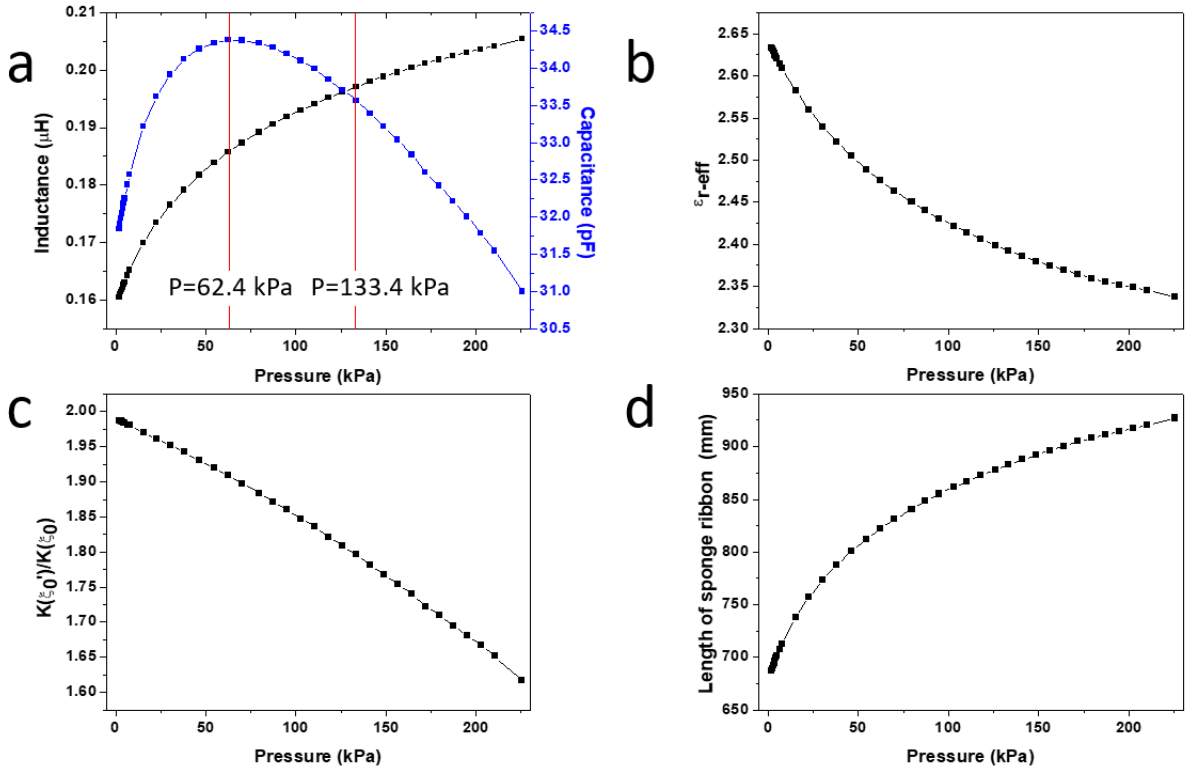

Figure S7 (a) Theoretical inductance and capacitance versus pressure for the sponge antenna encapsulated in Ecoflex. The inductance and capacitance were calculated based on equations #4 and #5 in the main body. (b) Theoretical ε_{r-eff} versus pressure. The ε_{r-eff} is calculated based on equations #11, #12 and #13 in Note S2. (c) Theoretical $K(\xi_0')/K(\xi_0)$ versus pressure. This value is calculated based on equations #9, #12 and #13 in Note S2. (d) Theoretical sponge ribbon length versus pressure. This length is calculated based on Poisson effect after calculating the compression ratio of sponge antenna's thickness.

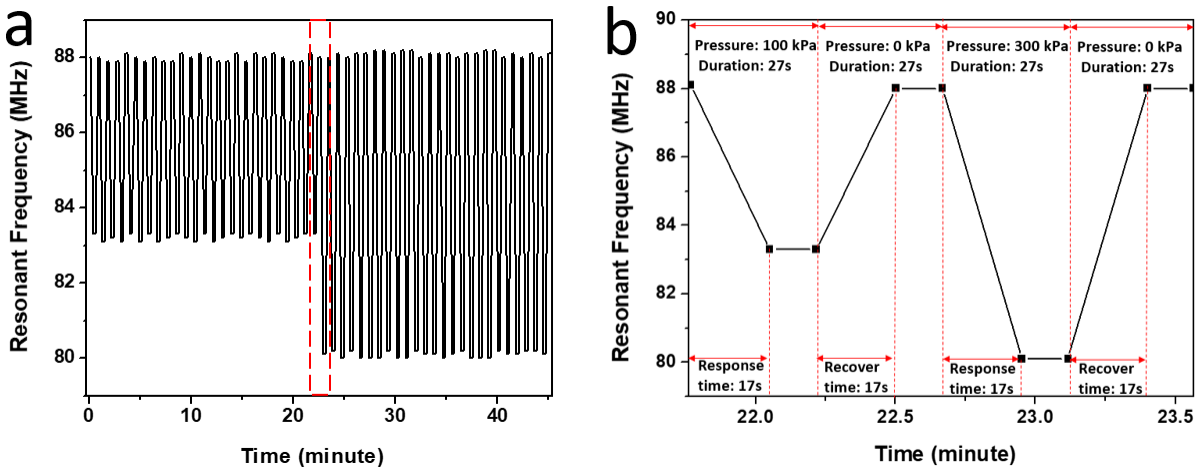

Figure S8 (a) Durability test for the sponge antenna encapsulated in PDMS. The mixing ratio of base and curing agent is 30:1 and the sponge thickness is 8.5 mm. 100 kPa and 300 kPa pressure were applied to the antenna for 25 cycles, respectively. During every cycle, static pressure was kept applying to the antenna for 27 s and then removed for 27 s. In the 27 s, 17 s is for adequate response time for network analyser and 10 s is for obtaining stable resonant frequency. (b) Magnified view of (a).

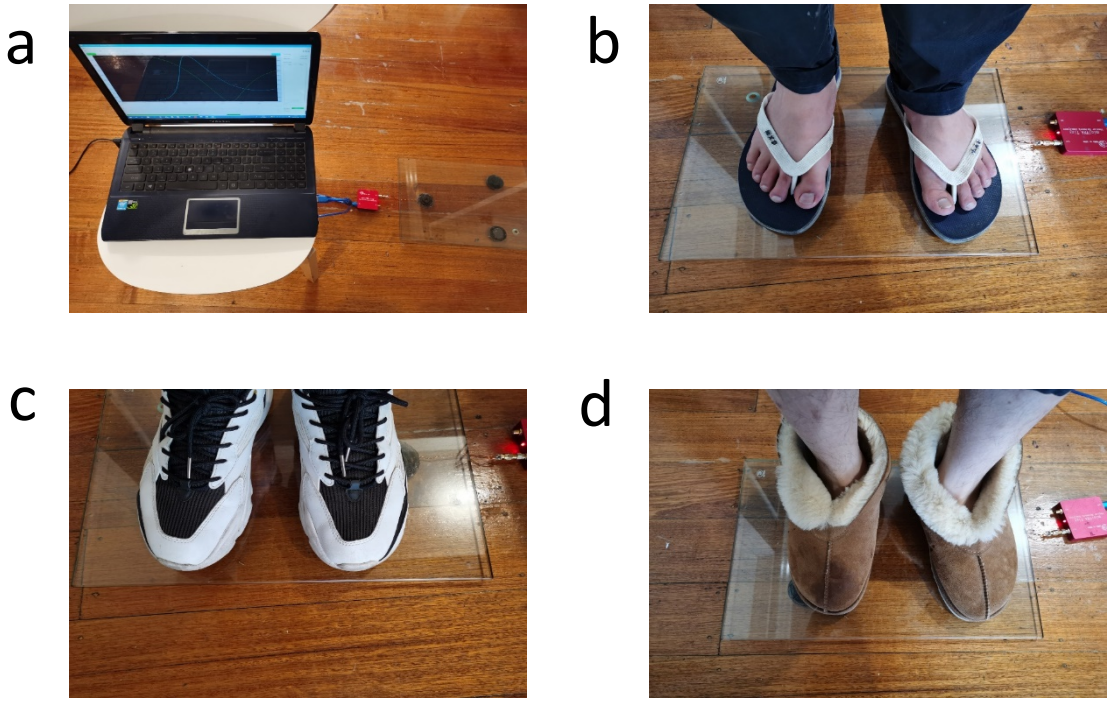

Figure S9 Proof of concept for sponge antenna as soft balance. (a) Experiment setup. (b)-(d) Three volunteers with weight of 61.3, 66.7 and 80.7 kg stood on the balance, respectively.

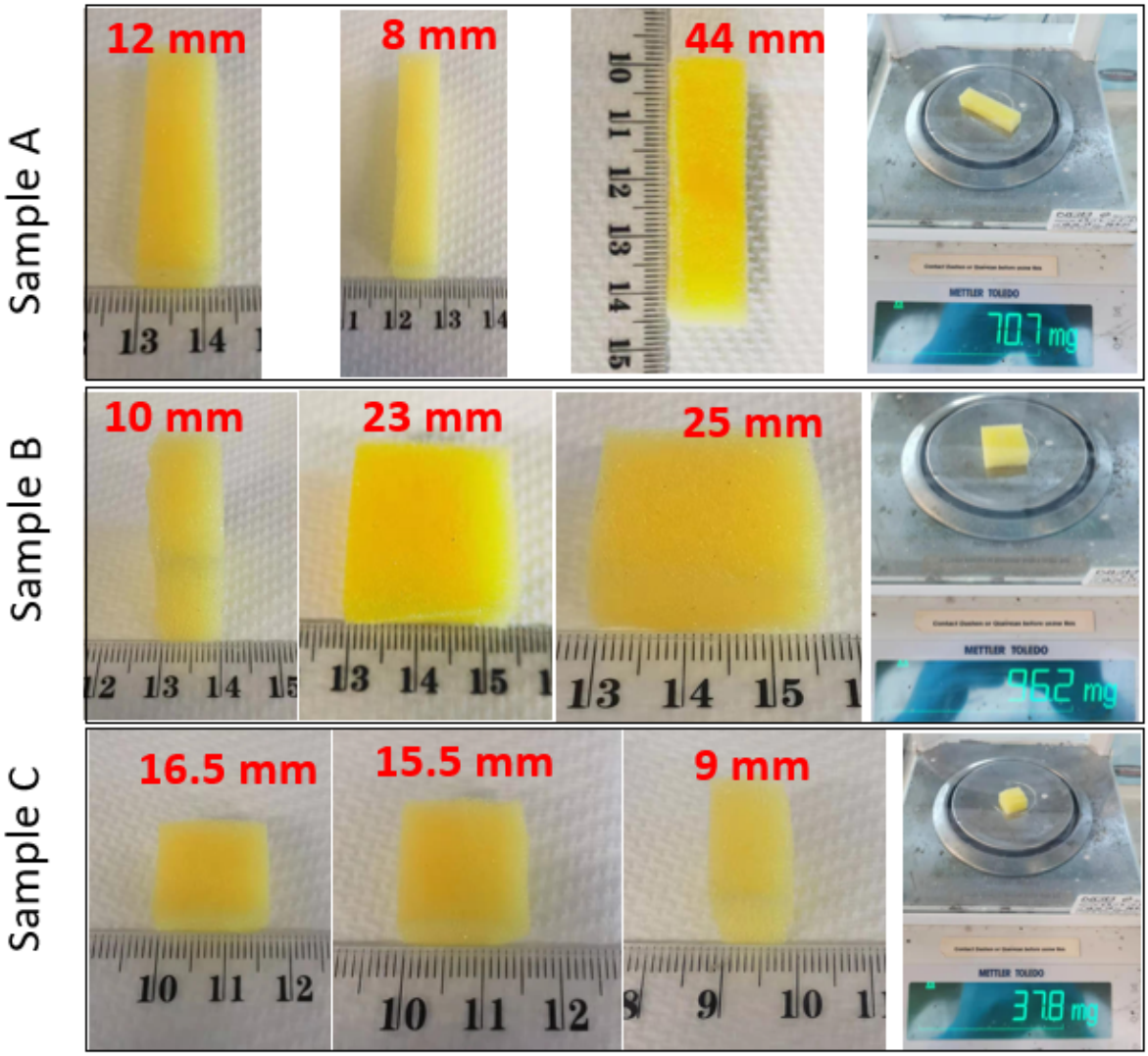

Figure S10 Dimension and weight of three pristine sponge samples for calculating the sponge's density.

Sample A: V=12*8*44=4224 mm^3

$\rho = \frac{m}{V} \approx 16.74\ kg/m^3$

Sample B: V=10*23*25=5750 mm^3

$\rho = \frac{m}{V} \approx 16.73\ kg/m^3$

Sample C: V=16.5*15.5*9=2301.75 mm^3

$\rho = \frac{m}{V} \approx 16.42\ kg/m^3$

Average density is (16.74+16.73+16.42)/3=16.63 kg/m^3

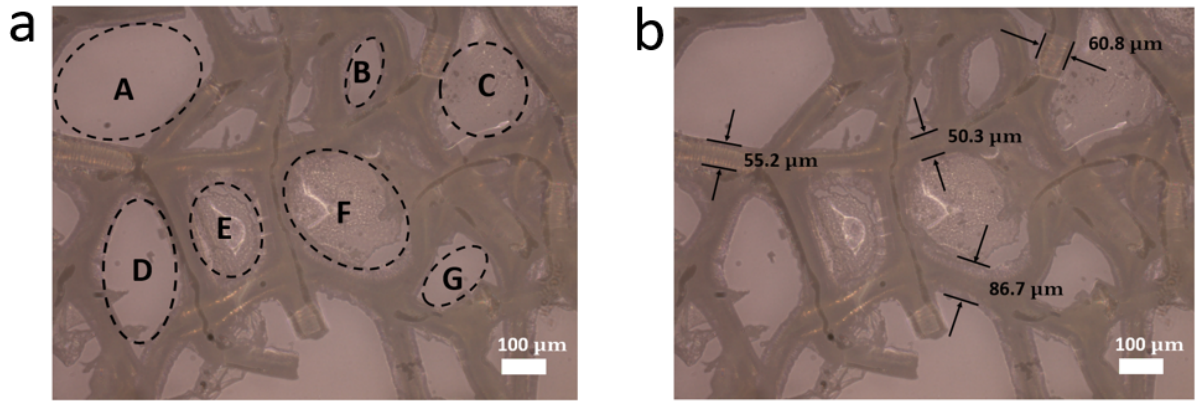

Figure S11 Microscope image of pristine sponge sample for calculating the pore size and skeleton width. (a) The ellipses from A to G represent the pores inside sponge. (b) The marked numbers represent the sponge skeleton's width at different positions.

For Figure S11a, the size of pores from A to G are

	A	B	C	D	E	F	G
2a (µm)	344.20	162.43	213.26	327.62	216.57	320.44	175.14
2b (µm)	250.28	75.14	199.45	165.75	159.67	229.83	95.58
area (mm2)	0.068	0.010	0.033	0.043	0.027	0.058	0.013

Therefore, the average area of pores is 0.039 ± 0.029 mm^2.

As shown in Figure S11b, the average size of sponge skeleton's width is 68.5 ± 18.2 µm.

Note S1

The real and imaginary part of Z_{in} can be measured by the network analyzer. They can also be calculated by

$$R_e\,(Z_{in}) = 2\pi f L_0 k^2 Q \frac{\frac{f}{f_s}}{1 + Q^2(\frac{f}{f_s} - \frac{f_s}{f})^2} \quad (1)$$

$$I_m\,(Z_{in}) = 2\pi f L_0 \left[1 + k^2 Q^2 \frac{1 - \left(\frac{f}{f_s}\right)^2}{1 + Q^2\left(\frac{f}{f_s} - \frac{f_s}{f}\right)^2}\right] \quad (2)$$

The phase $\angle Z_{in}$ can be expressed as

$$\angle Z_{in} = \arctan\frac{I_m\,(Z_{in})}{R_e\,(Z_{in})} \quad (3)$$

By solving the equation:

$$\frac{\partial \angle Z_{in}}{\partial f} = 0 \quad (4)$$

The frequency where the minimum phase of impedance occurs can be obtained by

$$f_{phase-dip} = (1 + \frac{1}{4}k^2 + \frac{1}{8Q^2})f_s \quad (5)$$

where k is the coupling coefficient for characterizing the interaction efficiency between the reader coil and the sponge antenna, which has a value in the range of 0 and 1;[2] Q is the antenna's quality factor, which is the ratio of f_{min} and the -3 dB bandwidth in the phase-frequency spectrum. Based on our sponge antennas, Q has a typical value of >5. Therefore, the second and third terms in the bracket approach zero. Thus, the equation that $f_{phase-dip} \approx f_s$ can be used for the analysis of gold sponge antenna.[2,3]

Note S2

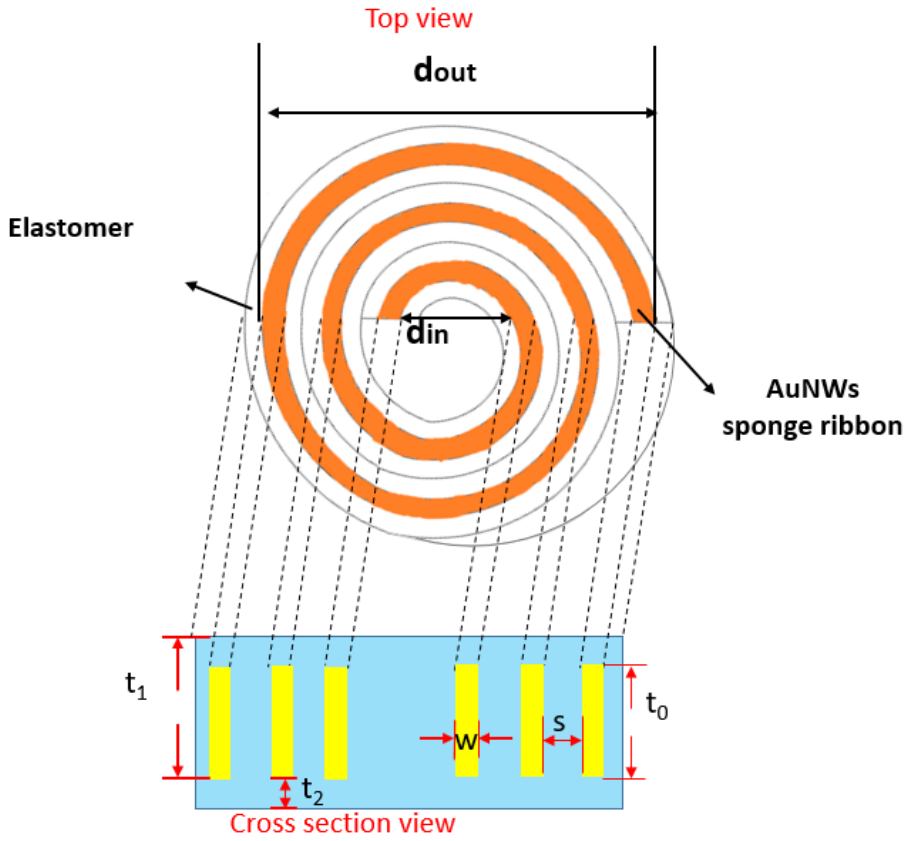

According to the scheme shown above, the inductance L_s can be written as[4]

$$L_s = \frac{\mu_0 \mu_r N^2 d_{avg}}{2} \left(\ln\left(\frac{2.46}{\rho}\right) + 0.2 * \rho^2\right) \quad (6)$$

where $\mu_0 = 4\pi \times 10^{-7}$ H/m, μ_r is the relative permeability. N is the turns of the sponge ribbon, $d_{avg} = 0.5(d_{out} + d_{in})$, $\rho = (d_{out} - d_{in})/(d_{out} + d_{in})$, d_{out} is the outer diameter and d_{in} is the inner diameter of the sponge antenna.

For our sponge antenna, N=8.5, therefore, $d_{out} = d_{in} + 18w + 16s$, $d_{avg} = d_{in} + 9w + 8s$, $\rho = \frac{9w+8s}{d_{in}+9w+8s}$.

When pressure is applied, we measured the compressed height of sponge antenna for calculating compression ratio of thickness. Following the rule of Poisson effect, we can obtain the elongation ratio of w and s, which is a half of the compression ratio. Put the changed w and s into the equation of d_{avg} and ρ, we can get the relationship between d_{avg}, ρ and pressure.

Consequently, the relationship between L_s and external pressure can be obtained. As shown in Figure S7a, The L_s kept increasing when pressure increased.

The capacitance C_s can be calculated by[5]

$$C_s = l * C_{ext} \quad (7)$$

$$C_{ext} = \varepsilon_{r-eff} C_0 \quad (8)$$

$$C_0 = \varepsilon_0 * \frac{K(\xi_0')}{K(\xi_0)} \quad (9)$$

$$C_s = l * \varepsilon_0 * \varepsilon_{r-eff} * \frac{K(\xi_0')}{K(\xi_0)} \quad (10)$$

$$\varepsilon_{r-eff} = 1 + \frac{1}{2}(\varepsilon_{r1} - 1)\frac{K(\xi_0)K(\xi_1')}{K(\xi_0')K(\xi_1)} + \frac{1}{2}(\varepsilon_{r2} - 1)\frac{K(\xi_0)K(\xi_2')}{K(\xi_0')K(\xi_2)} \quad (11)$$

$$\xi_i = \frac{\tanh(\frac{\pi s}{4t_i})}{\tanh(\frac{\pi(s+2w)}{4t_i})} \quad (12)$$

$$\xi_i' = \sqrt{1 - \xi_i^2} \quad (13)$$

where $\varepsilon_{r1} = \varepsilon_{r2} = 2.8$ for sponge antenna. K(ξ) is the complete elliptic integral of the first kind, the value for i is 0, 1 and 2.

C_s is affected by *l*, *s*, *w* and *t*, which are related to pressure. At first, we measured the compressed height and calculated the compression ratio of *t*. Following the rule of Poisson effect, we can obtain the elongation ratio of *l*, *s* and *w*, which is a half of the compression ratio. Therefore we can confirm the relationship between *l*, *s*, *w*, *t* and pressure. Then by using equations #11, #12 and #13, we can get the relationship between ε_{r-eff} and pressure (Figure S7b); by using equations #9, #12 and #13, the relationship between $\frac{K(\xi_0')}{K(\xi_0)}$ and pressure can be obtained (Figure S7c). After putting ε_{r-eff} and $\frac{K(\xi_0')}{K(\xi_0)}$ into equation #10, we can confirm the relationship between C_s and external pressure. As shown in Figure S7a, along with the increase of pressure, the C_s increases first and then decreases.

Table S1 The comparison on the linear detection range of wireless pressure sensing technologies.

Reference	Sensing mechanism	Linear detection range (kPa)
6	Capacitive	0-26.7
7	Capacitive	0-0.4
8	Capacitive	0-24
9	Capacitive	0-26.7
10	Capacitive	0-10
11	Inductive	0-14.6
12	Inductive	0-8
1	Inductive	0-20
13	Inductive-capacitive	0-4
This work	Inductive-capacitive	0-248

References

1 B. Nie, R. Huang, T. Yao, Y. Zhang, Y. Miao, C. Liu, J. Liu and X. Chen, *Adv. Funct. Mater.*, 2019, **29**, 1–10.

2 X. Huang, Y. Liu, H. Cheng, W. Shin, J. A. Fan, Z. Liu, C. Lu, G. Kong, K. Chen, D. Patnaik, S. Lee, S. Hage-ali, Y. Huang and J. A. Rogers, *Adv. Funct. Mater.*, 2014, **24**, 3846–3854.

3 T. J. Harpster, B. Stark and K. Najafi, *Sensors Actuators, A Phys.*, 2002, **95**, 100–107.

4 Q. Tan, T. Luo, J. Xiong, H. Kang, X. Ji, Y. Zhang, M. Yang, X. Wang, C. Xue, J. Liu and W. Zhang, *Sensors (Switzerland)*, 2014, **14**, 4154–4166.

5 Q. A. Huang, L. Dong and L. F. Wang, *J. Microelectromechanical Syst.*, 2016, **25**, 822–841.

6 A. Palmroth, T. Salpavaara, P. Vuoristo, S. Karjalainen, T. Kääriäinen, S. Miettinen, J. Massera, J. Lekkala and M. Kellomäki, *ACS Appl. Mater. Interfaces*, 2020, **12**, 31148–31161.

7 R. Wu, L. Ma, A. Patil, C. Hou, S. Zhu, X. Fan, H. Lin, W. Yu, W. Guo and X. Y. Liu, *ACS Appl. Mater. Interfaces*, 2019, **11**, 33336–33346.

8 J. Park, J. K. Kim, D. S. Kim, A. Shanmugasundaram, S. A. Park, S. Kang, S. H. Kim, M. H. Jeong and D. W. Lee, *Sensors Actuators, B Chem.*, 2019, **280**, 201–209.

9 A. Palmroth, T. Salpavaara, J. Lekkala and M. Kellomäki, *Adv. Mater. Technol.*, 2019, **4**, 1900428.

10 G. H. Lee, J. K. Park, J. Byun, J. C. Yang, S. Y. Kwon, C. Kim, C. Jang, J. Y. Sim, J. G. Yook and S. Park, *Adv. Mater.*, 2020, **32**, 1906269.

11 C. I. Jang, K. S. Shin, M. J. Kim, K. S. Yun, K. H. Park, J. Y. Kang and S. H. Lee, *Appl. Phys. Lett.*, , DOI:10.1063/1.4943136.

12 Y. W. Kim, M. J. Kim, K. H. Park, J. W. Jeoung, S. Hwan, C. In, J. Ms, S. H. Lee, J. H. Kim, S. Lee and J. Yoon, *Clin. Exp. Ophthalmol.*, 2015, 830–837.

13 P. J. Chen, D. C. Rodger, S. Saati, M. S. Humayun and Y. C. Tai, *J. Microelectromechanical Syst.*, 2008, **17**, 1342–1351.